Excitonic properties of ZnS quantum wells

B. Urbaszek,[1] C. M. Townsley,[2] X. Tang,[1] C. Morhain,[1] A. Balocchi,[1] K. A. Prior,[1] R. J. Nicholas,[2] and B. C. Cavenett[1]
[1]*Department of Physics, Heriot-Watt University, Edinburgh EH14 4AS, United Kingdom* [2]*Clarendon Laboratory, Department of Physics, University of Oxford, Parks Road, Oxford OX1 3PU, United Kingdom*
(Received 1 May 2001; published 25 September 2001)

The excitonic properties of cubic ZnS quantum wells in ZnMgS are studied by reflectivity and magneto-optics. A remarkable improvement in the quality of the samples grown by molecular-beam epitaxy on GaP substrates has allowed the observation of heavy- and light-hole exciton transitions with values for the full width at half maximum as narrow as 5 meV. The 2*s* state of the heavy-hole exciton is identified and exciton binding energies of as high as 55 meV are deduced, indicating that for quantum wells narrower than 3.5 nm the exciton-LO phonon scattering can be suppressed. Zeeman splittings of the order of 10 meV for both the light- and heavy-hole exciton transitions appear in magnetoreflectivity spectra in magnetic fields up to 54 T. Large light-hole exciton *g* values of the order of 4 for all quantum wells are obtained due to the light hole being the uppermost valence band in these tensile-strained quantum wells. A strong reduction in the diamagnetic shifts for narrow wells is observed due to increasing quantum confinement.

DOI: 10.1103/PhysRevB.64.155321 PACS number(s): 73.63.Hs, 71.35.−y, 78.66.Hf, 71.35.Ji

I. INTRODUCTION

With a room-temperature band gap of 3.7 eV, ZnS and its alloys are of interest for UV applications, but a key factor for high-performance optoelectronic devices is the stabilization of excitons at room temperature since, for example, excitonic gain in lasers is much higher than that associated with a free-electron-hole plasma and so should allow low-threshold laser emission. Also, an enhancement of the excitonic absorption and a narrowing of the line width at room temperature is important for the design of modulators. Laser emission due to excitonic and biexcitonic gain mechanisms have been observed in ZnSe-based structures by several groups[1,2] for temperatures up to 150 K. However, the strong interaction between the excitons and LO phonons usually results in the dissociation of the excitons at higher temperatures, reducing device efficiencies, and so it is important to suppress the exciton-LO phonon scattering. In particular, ionization of excitons should be prevented in systems where all the excitations of the exciton have an energy larger than that of the LO phonon, namely, for $E^X(1s-2s)>h\nu_{\mathrm{LO}}$, due to the absence of final states for the scattering process.[3] In the case of ZnS the bulk exciton binding energy is 36 meV compared with an LO phonon energy of 44 meV and so in quantum well structures where the exciton binding energy is typically enhanced by a factor of 1.5–2 due to quantum confinement this condition should be achievable. Also, since the lattice mismatch of ZnS on GaP substrates is only 0.76% and ZnMgS can be grown lattice matched to GaP, the ZnMgS/ZnS/ZnMgS quantum well is an ideal system to explore the possibility of suppressing the exciton-LO phonon scattering. The use of ZnS as a binary material has the advantage that alloy broadening in the structures is confined to the barrier layers.

In this paper, we present a detailed spectroscopic study of a set of high-quality ZnMgS/ZnS/ZnMgS quantum wells where the ZnS is under tensile strain and the ZnMgS barriers are lattice matched to the GaP substrate. The full widths at half maximum of the optical transitions are as narrow as 5 meV in the reflection spectra, allowing the observation of both light- and heavy-hole exciton ground states for quantum well widths ranging from 3.5 to 10.0 nm. A spectral feature on the high-energy side of the heavy-hole 1*s* exciton is attributed to the heavy-hole 2*s* exciton state, giving a first indication of the exciton binding energies in this material system. The excitonic properties of these structures have been investigated by magnetoreflectivity in pulsed fields up to 54 T and a splitting of both light- and heavy-hole 1*s* exciton states in the order of 10 meV was observed. The exciton *g* values were measured and the deduced diamagnetic shift was used to study the role of quantum confinement.

II. GROWTH, PHOTOLUMINESCENCE, AND X RAY

All the samples investigated here were grown by molecular-beam epitaxy (MBE) in a VG V80H system using 6N sources of Zn, Mg, ZnS, and S. GaP (100) n^+ substrates were etched *ex situ*, transferred to the MBE system, and the oxide layer was removed between 580° and 630 °C while the sample was exposed to a zinc flux. Using this procedure the (2×4) reconstruction was routinely observed by reflection high-energy electron diffraction on cooling the sample to the growth temperature, typically 170 °C. During the growth of the ZnMgS layers only ZnS and Mg fluxes were used; there was no other source of sulphur.[4] Typical cell temperatures were 770 °C for ZnS and 270°–290 °C for Mg.

We investigated ZnS quantum wells in ZnMgS barriers lattice matched to GaP substrates. The high optical and structural qualities of the samples were demonstrated in the photoluminescence (PL) and in the double-crystal x-ray rocking curves (DCXRD). In fact, both the PL line widths and DCXRD data were significantly better than had been obtained previously,[6,5] which we attribute to the fact that these samples were grown pseudomorphically on GaP, whereas earlier samples were grown on relaxed buffers of ZnS.

The PL measurements were carried out using a 0.75-m Spex monochromator equipped with a 1200-lines/mm grat-

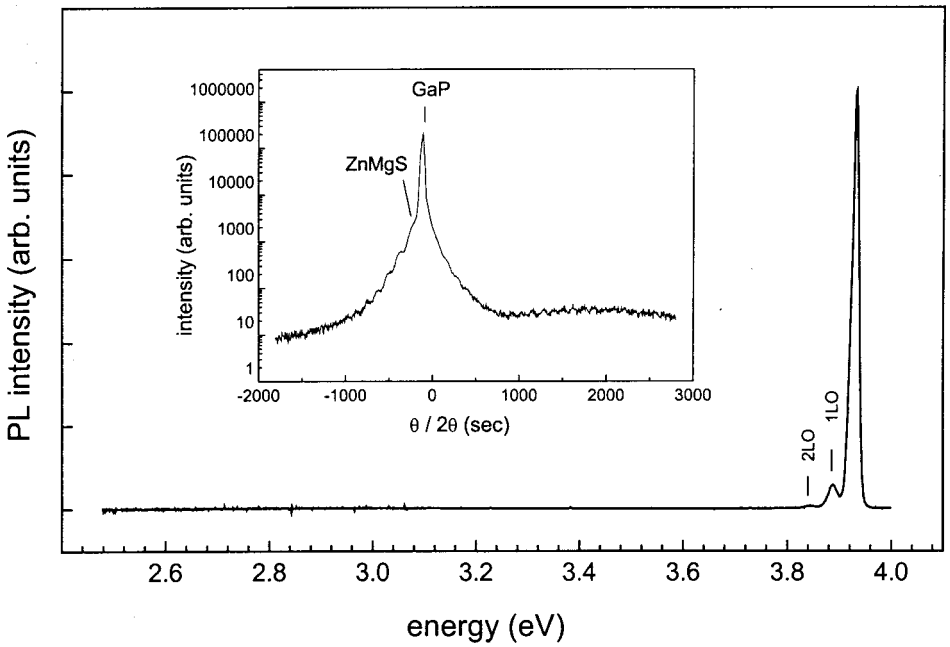

FIG. 1. 4-K photoluminescence spectrum of a $Zn_{0.86}Mg_{0.14}S$ sample grown on GaP (100). Inset: DCXRD spectra for samples with structures ZnMgS (150)/ZnS (10)/ZnMgS (150 nm).

ing and recorded using a photomultiplier tube and excitation from an Argon ion laser using the 275–300-nm lines with excitation densities of typically 1 W cm^{-2}. For the reflection spectroscopy described in Sec. III a deuterium lamp was used. The PL spectrum of a $Zn_{0.86}Mg_{0.14}S$ sample in Fig. 1 clearly shows one strong emission line, accompanied by several LO phonon replicas, and there is virtually no deep level emission. The full width at half maximum (FWHM) of the intense PL line is 15 meV, which is reduced to 11 meV in a sample containing a mole fraction of only 7% magnesium. DCXRD spectra are shown the inset of Fig. 1 for a sample containing one 10-nm-wide quantum well. In this sample the ZnMgS layer is almost lattice matched to the GaP substrate and the narrow FWMH is indicative of good crystallinity.

A set of quantum wells was grown with quantum well widths of 10, 5, 4, and 3.5 nm with the number of quantum wells being one, two, four, and four respectively. The well width ranged from 4 to 1.4 times the ZnS exciton Bohr radius ($a_B = 2.5$ nm) thus going from bulklike to strong spatial confinement. The number of quantum wells was reduced in the wider wells to ensure that the critical thickness of $t_c \approx 25$ nm, calculated with the model of Dunstan *et al.*,[6] for ZnS under tensile strain with unstrained $Zn_{1-x}Mg_xS$ ($x = 19\%$) barriers, was not exceeded. The Mg content of 19% as determined by x ray is the same for all samples and was used in all calculations in the following sections.

The tensile strain causes a reduction in the ZnS band gap and the valence band is split into separate heavy- and light-hole bands. The light-hole energy is moved upward and the heavy-hole energy downward, opposing the effect of quantum confinement. It is therefore possible to design structures with either the light or heavy hole being the uppermost valence band. For ZnS in $Zn_{0.81}Mg_{0.19}S$ the light-hole exciton is the energetically lowest transition for wells wider than 2 nm, as for all samples investigated.

At zero strain the spin-orbit split-off (SO) band is separated from the degenerate light- and heavy-hole bands by an energy of only 70 meV in ZnS, as compared to 430 meV in ZnSe. At finite strain the proximity of the SO band means that it should also be taken into account in the coupling of the valence bands. The following relations are used to describe the shift of the band-edge energies with strain:[7]

$$\varepsilon_{xx} = \varepsilon_{yy} = \frac{a_0 - a}{a},$$

$$\varepsilon_{zz} = -\frac{2C_{12}}{C_{11}}\varepsilon_{xx}, \tag{1}$$

$$P_\varepsilon = -a_\nu(2\varepsilon_{xx} + \varepsilon_{zz}),$$

$$Q_\varepsilon = -b(\varepsilon_{xx} - \varepsilon_{zz}). \tag{2}$$

The band-edge energies at the center of the first Brillouin zone ($k = 0$) are

$$E_{\mathrm{HH}}(0) = -P_\varepsilon - Q_\varepsilon,$$

$$E_{\mathrm{LH}}(0) = -P_\varepsilon + \tfrac{1}{2}[Q_\varepsilon - \Delta + (\Delta^2 + 2\Delta Q_\varepsilon + 9Q_\varepsilon^2)^{1/2}],$$

$$E_{\mathrm{SO}}(0) = -P_\varepsilon + \tfrac{1}{2}[Q_\varepsilon - \Delta - (\Delta^2 + 2\Delta Q_\varepsilon + 9Q_\varepsilon^2)^{1/2}], \tag{3}$$

where a_0 and a are the lattice constants of the barrier and the quantum well material, a_v and b are the deformation potentials, C_{12} and C_{11} are the elastic stiffness constants, and Δ is the energy separation of the split-off band at zero strain.

The coupling results in a change in band-edge energies since the light-hole and SO-band levels repel each other and the energy difference is increased from 70 to 100 meV; the heavy-hole band is not affected by the coupling at $k = 0$.

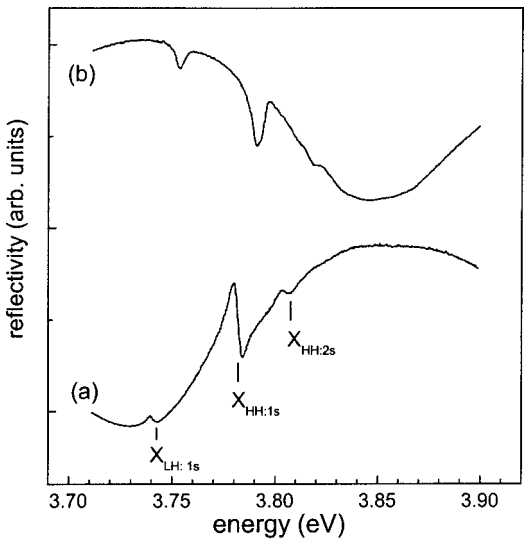

FIG. 2. 4-K reflectivity spectra of (a) 10- and (b) 5-nm ZnS quantum wells.

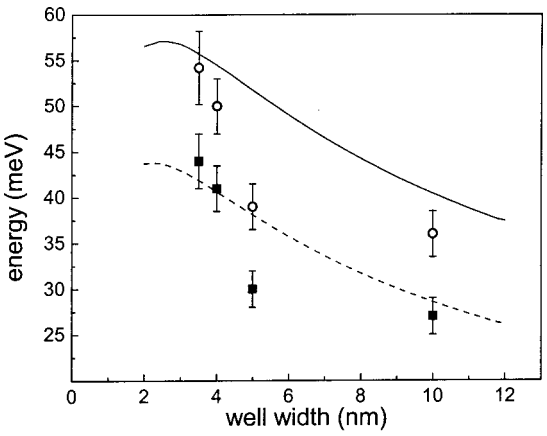

FIG. 3. Measured energy separation between the 1*s* to 2*s* heavy-hole exciton states (solid squares) and the 1*s* exciton binding energy derived from the measurement (hollow circles) using Ref. 8. The calculated 1*s* exciton binding energies (solid line) and the energy separations between the 1*s* to 2*s* heavy-hole exciton states (dashed line) are shown for comparison using the model in Ref. 9. Note the LO-phonon energy in ZnS of 44 meV.

III. REFLECTIVITY EXCITON SPECTRA

The effect of increasing confinement on the exciton transitions in going from 10 to 3.5-nm well width was measured by reflectivity. Reflectivity spectra for the 10 and 5-nm quantum wells are shown in Figs. 2(a) and 2(b) respectively, where three different quantum well transitions are clearly observed, superimposed on interference oscillations up to an energy of 4.0 eV, which is the band gap of the barrier layers. The exciton spectral features in the reflectivity appear in either derivative or absorptive form depending upon their position relative to the overall interference pattern and it can be seen that for the 10-nm well the sharp excitonic features due to the well appear as derivatives, while for the 5-nm well the features correspond directly to minima. In all four samples three features are observed, which are attributed to the light-hole (LH) 1*s* exciton and the 1*s* and 2*s* exciton features of the heavy hole (HH). The HH exciton features are stronger than those from the light-hole exciton features due to the larger oscillator strength of the HH exciton, while the 2*s* feature is approximately five times weaker than the 1*s*. Any 2*s* feature from the LH is close to the noise level but can be very weakly observed when a magnetic field is applied. The observation of a clearly resolved 2*s* state is particularly crucial in enabling us to determine the excitonic Rydberg in this system.

We have used the analytic method of Mathieu, Lefebvre, and Christol[8] to calculate the value of the excitonic Rydberg from the measured value of $E^X(1s-2s)$ for the HH exciton as a function of well width. As can be seen in Fig. 3 it is just possible to achieve the condition $E^X(1s-2s)>h\nu_{\mathrm{LO}}$ for heavy-hole excitons for quantum wells narrower than 3.5 nm. In order to compare these data with theoretical predictions we have calculated the exciton binding energy using the model of Peyla *et al.*[9] These calculations are strongly dependent on the material parameters for ZnS, which are not as well known as for many other II-VI and III-V semiconductors. The difference in band gap between the ZnMgS barrier material and the strained ZnS quantum well is taken to be evenly distributed between valence and conduction bands.[5] This amounts to valence-band offsets of 87 meV for the heavy hole and 106 meV for the light hole. We have used an electron effective mass of $0.34m_e$ reported by Kukimoto *et al.*,[10] and for the in-plane reduced mass we have used the approximation first proposed by Baldareschi and Lipari[11] of $m_h=1/\gamma_1$ for bulk materials. In the present case the LH and HH are significantly decoupled, which might lead us to expect that the HH in-plane mass should be significantly reduced, however, recent calculations on similar ZnSe-based heterostructures[12] suggest that this is not the case, due to the large contribution to the hole properties from large *k* sections of the dispersion relation where the HH and LH bands are strongly mixed. We therefore use the bulk approximation that gives a reduced mass $\mu=0.181$, which is around 10% higher than the values deduced for ZnSe, which has a band gap approximately 10% less than ZnS. Using these values we find excellent agreement with the measured Rydberg values shown in Fig. 3.

IV. MAGNETOREFLECTIVITY

Magneto-optics is a well-established technique to investigate the excitonic properties of semiconductor quantum wells. The magnetic-field dependencies of the ground states are described by the Zeeman effect and a diamagnetic shift. Information about the band structure can be obtained from effective exciton *g* values and exciton wave functions are measurable through the diamagnetic coefficient. The higher excited states of the excitons such as the 2*s* transitions increase in oscillator strength when a magnetic field is applied parallel to the growth direction (Faraday geometry). The transitions can then become more clearly detectable in the spectra allowing the direct determination of the zero-field exciton binding energy.[13]

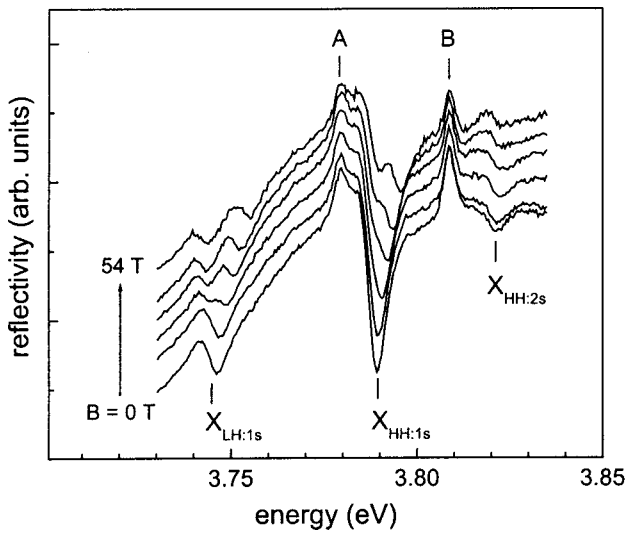

FIG. 4. Enlarged reflectivity of a 5-nm ZnS quantum well sample in ZnMgS for light- ($X_{\mathrm{LH:1}s}$) and heavy-hole ($X_{\mathrm{HH:1}s}$ and $X_{\mathrm{HH:2}s}$) exciton transitions for magnetic fields from 0 to 53.5 T. Spectral feature of the Xe-flash lamp are marked as A and B.

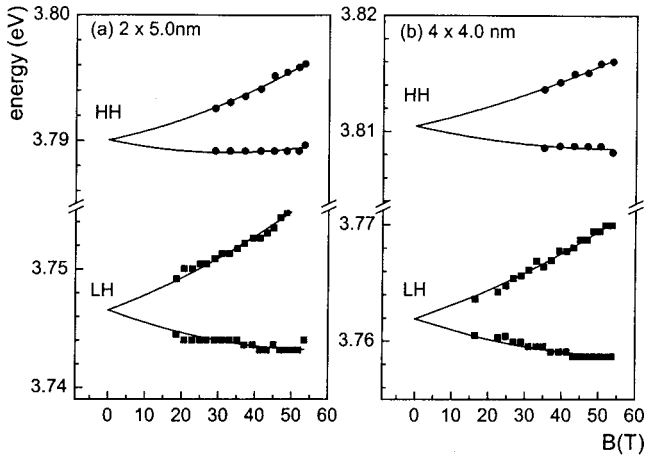

FIG. 5. The symbols indicate the measured transition energies for the light- (LH) and heavy-hole (HH) exciton transitions for the 5-and 4-nm ZnS quantum wells. The solid lines are the fits obtained with Eq. (4).

The improvement in the material quality as described in the first part of this study was essential to allow the observation of the changes in the reflectivity spectra induced by the magnetic field. To date, to the best of our knowledge, magneto-optical data only exist for bulk ZnS samples; no experiments have been previously reported for ZnS quantum wells. The large effective masses in the system do, however, require the use of very high magnetic-field values in order to achieve resolvable splittings. This, therefore, necessitated the use of pulsed magnetic fields up to 54 T at the Oxford pulsed magnetic-field facility. The samples were immersed in liquid helium (4.2 K) in the bore of a liquid-nitrogen-cooled resistive magnet through which was passed the energy stored in an 8-μF bank of capacitors, charged up to ~5000 V. A xenon-flash lamp was used as a white-light source and was fired at the peak field. The signal was detected with a charge-coupled device (CCD) camera and the resulting spectra were then normalized against a mirror to attempt to eliminate most of the background features from the Xe lamp, although some small spikes, which were independent of field, can be seen in some of the spectra.

Figure 4 shows the magnetoreflectivity from the 15-nm quantum well in the region of the LH-1*s*, HH-1*s*, and HH-2*s* peaks. The behavior is typical for all of the samples studied in which both the 1*s* peaks show a well-resolved spin splitting above ~25 T. In order to analyze the peak positions as accurately as possible we use the first derivative of the reflectivity spectra.

Although the magnetic fields used are very high, the relative field strength for ZnS of 50 T is comparable to 1.5 T in GaAs due to the difference in carrier masses and bulk exciton binding energies. Because of the small relative field strength the effects of additional band mixing introduced by the magnetic field that could contribute nonlinearly to the Zeeman splitting can still be ignored.[14] The exchange interaction of the quantum well ground-state transitions is also assumed to be negligible, as no level anticrossing was observed.

The ground-state transition energies can thus be described by a sum of zero-field energy, diamagnetic shift, and Zeeman splitting:[13]

$$E(B) = E_i + \delta B^2 \pm \tfrac{1}{2}\, g_{\mathrm{eff}} \mu_B B, \tag{4}$$

where E_i stands for the $E1\mathrm{LH}1$ and $E1\mathrm{HH}1$ transitions, δ is the diamagnetic shift parameter, and μ_B is the Bohr magneton. Figure 5 shows the ground-state transitions for the HH and LH as a function of the applied field for a 5- and a 4-nm-wide ZnS quantum well.

The effective exciton g values measured for both LH and HH excitons are summarized in Table I. Both are quite large, with the LH value being larger than the HH for the range of well widths investigated. Our results are larger than the g values reported by Yamada *et al.*[15] for nonstrained bulk ZnS from PL measurements on biexcitons in magnetic fields up to 9 T. This behavior is the result of the splitting of the LH and HH exciton states due to the tensile strain in the ZnS well, resulting in the LH being the uppermost valence band. As a result the ordering of the LH spin states is reversed leading to a Zeeman splitting for the exciton where the splittings of the electrons and holes are additive. This can be modeled quite simply using the Luttinger approach[16] in which the exciton Hamiltonian takes the form

TABLE I. Effective exciton g factors and diamagnetic parameters for heavy- and light-hole excitons in ZnS quantum wells.

Well width (nm)	g_{eff} (HH)	δ (HH) (μeV/T^2)	g_{eff} (LH)	δ (LH) (μeV/T^2)
3.5			4.22	0.50
4.0	2.20	0.65	3.87	0.89
5.0	1.97	0.96	3.79	1.00
10.0	3.13	1.56	3.82	1.55

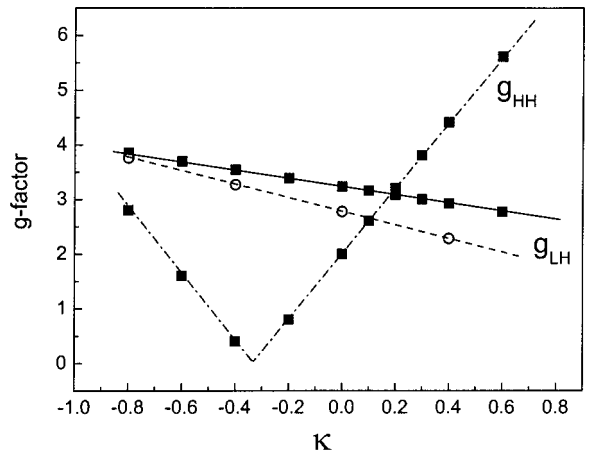

FIG. 6. Calculated effective g values for light- and heavy-hole excitons as a function of the parameter κ for ZnS quantum wells under tensile strain in ZnMgS. Values are shown for two different values of the splitting parameter Δ_{cf} ($\Delta_{cf}=40$ meV—solid line, $\Delta_{cf}=20$ meV—dashed line) for the LH. The g value for the HH does not depend on Δ_{cf} (dash-dotted line).

$$H_0=E_0+H_B-\Delta_{cf}l_z^2-\tfrac{2}{3}\Delta_{SO}\boldsymbol{l}\cdot\boldsymbol{s}$$

with

$$H_B=g_e\mu_B\boldsymbol{B}\cdot\boldsymbol{s}_e+2\mu_B\boldsymbol{B}\cdot\boldsymbol{s}-\mu_B(3\kappa+1)\boldsymbol{B}\cdot\boldsymbol{l}, \qquad (5)$$

where the first term in H_B corresponds to the Zeeman splitting of the conduction band and the next two terms describe the splitting from the spin and orbital angular momentum of the hole. The crystal-field term Δ_{cf} is responsible for the splitting of the HH and LH states due to the combination of strain and confinement effects. A similar approach has been used in the modeling of GaN (Ref. 17), which is very similar to ZnS with an even smaller spin-orbit splitting and with a splitting of the HH and LH caused by the wurzite band structure. The situation is different for the HH exciton; the contribution of HH and conduction-band electrons partially cancel each other out. Indeed the similarity with GaN is even more striking since recent measurements by Shields *et al.*[18] in AlGaN/GaN quantum wells have found similarly large g factors, which are attributed also to strain-induced reversal of the quasi-HH (A) and quasi-LH (B) bands. Using an effective g value of 1.88 for the conduction-band electrons in nonstrained bulk ZnS,[19] we have calculated the HH and LH exciton splittings as a function of the band parameter κ as shown in Fig. 6. This shows that the large value of the LH g factor is well predicted by this approach, and that the HH g factor is very sensitively dependent on κ. The most reliable results are from the 10-nm-wide well as this has both the narrowest lines, the largest HH-LH splitting, and is the closest to bulk behavior. From this data we conclude that the value of κ of 0.17 originally proposed by Lawaetz[20] fits the data very well. The only surprising feature of our data when compared to the fitting is that the magnitude of the predicted HH g factor is almost independent of the LH-HH separation, whereas in practice we find that the HH exciton g factor is strongly reduced with decreasing well width. This may be due to the fact that we have not included exchange coupling, which is probably just becoming significant when the excitons are more strongly confined.

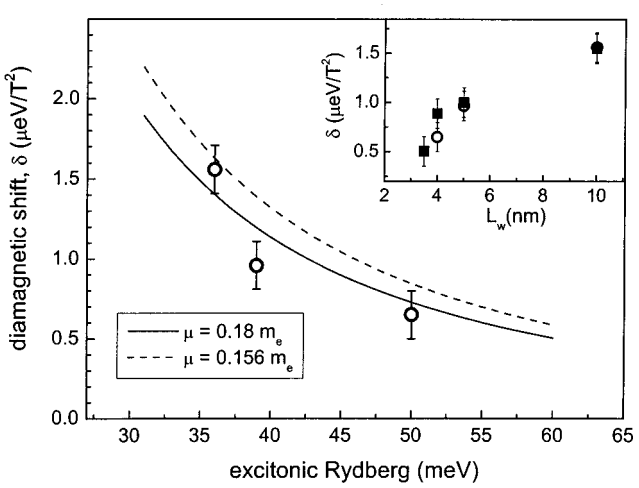

FIG. 7. Diamagnetic parameter δ as a function of the excitonic Rydberg for the LH and HH. The solid and dashed lines show the values predicted by Eq. (7) for the reduced mass values of 0.18 and $0.156m_e$. The excitonic Rydberg for the HH from the zero-field reflectivity is plotted for comparison. Inset: Measured diamagnetic parameter δ as a function of well width for the light- (solid squares) and heavy-hole (hollow circles) excitons.

We now turn to the diamagnetic shift parameter δ, which is a measure of the carrier confinement. Decreasing values of δ are expected for increasing confinement and indeed this trend could be seen quite clearly for both types of excitons in the samples investigated, as can be seen in Fig. 7. The diamagnetic shift in weak magnetic fields can be calculated by first-order perturbation theory[13,21] as

$$\Delta E_{\mathrm{dia}}=\delta B^2=\frac{e^2B^2}{8\mu}\langle\rho^2\rangle, \qquad (6)$$

where μ is the in-plane reduced exciton mass and ρ is the in-plane radius. Weak magnetic fields of $\gamma<0.4$ in ZnS correspond to $B<52$ T, where γ is defined as $\gamma=\hbar\omega_c/2Ry$ with ω_c and Ry being the cyclotron frequency and the bulk exciton binding energy, respectively. The spatial extension of an exciton reaches its minimum for maximum confinement. The value of $\langle\rho^2\rangle$ is expected to decrease with decreasing quantum well width until maximum confinement is reached. For even narrower wells, the value of $\langle\rho^2\rangle$ increases again as tunneling effects become important. For bulk the relation $\langle\rho^2\rangle=2a_B^2$ holds, whereas for purely two-dimensional (2D) excitons $\langle\rho^2\rangle=(3/8)a_B^2$, where a_B is the bulk exciton Bohr radius. The inset of Fig. 7 shows that there is a rapid decrease in the values of the diamagnetic shifts as a function of decreasing well width, consistent with both the increase in the exciton binding energy and the expected decrease in the exciton radius. In order to compare the observed diamagnetic shifts with the data on the excitonic Rydberg we can make the very approximate assumption that for well widths comparable to the excitonic Bohr radius a 3D approximation would be appropriate. This is justified mainly by the obser-

vation that the excitonic binding energies are considerably closer to the 3D than the 2D limit. In this case we may use expression (6) together with the conventional formulas for the effective Rydberg to show that

$$\delta=\left(\frac{1}{R^*}\right)^2\frac{1}{\mu}\left(\frac{e a_0^H R^H}{2\varepsilon_r}\right)^2, \tag{7}$$

where a_0^H and R^H are the full hydrogen values of the Bohr radius and Rydberg energy. This expression is plotted for ZnS in Fig. 7 using a dielectric constant of $\varepsilon_r=8.0$ and reduced effective-mass values of $\mu=0.18m_e$ as suggested by using the electron mass value of $0.34m_e$ and $\mu=0.156m_e$ deduced using the value of $0.26m_e$ for the electron mass reported by Miklosz and Wheeler.[22] The excitonic Rydberg predicted by Eq. (7) reproduces well the values obtained from the zero-field reflectivity in Sec. III for the HH. For both mass values the systematic trend is well described, the higher mass values giving better agreement.

Although higher excited exciton states were not clearly observed during the experiments, there are a few cases where features could be seen. For the 10-nm sample the highest-field traces showed detectable spin-split $2s$ features for the LH exciton which suggest that the LH binding energy is within 1–2 meV of that deduced for the HH, and that the g factor of the $2s$ state is the same as for the $1s$. By contrast the g factor deduced for the HH $2s$ is significantly lower ($\sim$2.0) than seen for $1s$. For all other samples the LH-$2s$ features overlapped the stronger HH-$1s$ state and could not be detected.

V. CONCLUSION

Reflectivity and magneto-optics were used to study the excitonic properties of high-quality ZnS quantum wells in ZnMgS. Heavy- and light-hole exciton transitions as narrow as 5 meV are observed for quantum wells with thicknesses ranging from 3.5 to 10 nm. The effective Rydberg has been measured and found to reach values as high as 55 meV, which enables the condition $E^X(1s-2s)>h\upsilon_{\mathrm{LO}}$ to be satisfied. It is therefore expected to observe suppression of exciton-LO phonon scattering for both light- and heavy-hole excitons in these samples. The magnetic-field dependencies of the light- and heavy-hole transitions was described as a sum of Zeeman effect and diamagnetic shift. The measured effective g factors are found to be very large due to the light-hole band being the topmost band in this tensile-strained system. The rapid reduction in diamagnetic shift for the narrow wells indicates the strong carrier confinement in these samples and is consistent with the observed increase in the excitonic effective Rydberg.

ACKNOWLEDGMENTS

We gratefully acknowledge the support of EPSRC and the ESPRIT EU program. C.M. is grateful for the support of the Société des Amis des Sciences and that of the EU through its TMR scheme.

[1] F. Kreller, M. Lowisch, J. Puls, and F. Henneberger, Phys. Rev. Lett. **75**, 2420 (1995).
[2] O. Homburg, P. Michler, R. Heinecke, J. Gutowski, H. Wenisch, M. Behringer, and D. Hommel, Phys. Rev. B **60**, 5743 (1999).
[3] S. Nojima, Phys. Rev. B **46**, 2302 (1992).
[4] K. A. Prior, S. A. Telfer, X. Tang, C. Morhain, B. Urbaszek, C. O'Donnell, P. Tomasini, A. Balocchi, and B. C. Cavenett, J. Crystal Growth **227-228**, 655 (2001).
[5] K. Ichino, K. Ueyama, H. Kariya, N. Suzuki, H. Miyata, M. Kitagawa, and H. Kobayashi, Appl. Phys. Lett. **74**, 3486 (1999).
[6] D. J. Dunstan, S. Young, and R. H. Dixon, J. Appl. Phys. **70**, 3038 (1991).
[7] C. Y. Chao and S. L. Chuang, Phys. Rev. B **46**, 4110 (1992).
[8] H. Mathieu, P. Lefebvre, and P. Christol, Phys. Rev. B **46**, 4092 (1992).
[9] P. Peyla, R. Romestain, Y. Merle d'Aubingé, G. Fishman, A. Wasiela, and H. Mariette, Phys. Rev. B **51**, 12 026 (1995).
[10] H. Kukimoto, S. Shionoya, T. Koda, and T. Hioki, J. Phys. Chem. Solids **29**, 935 (1968).
[11] A. Baldareschi and N. O. Lipari, Phys. Rev. B **3**, 439 (1971).
[12] J. Puls, M. Rabe, A. Siarkos, and F. Henneberger, Phys. Rev. B **57**, 14 749 (1998).
[13] J. Puls, V. V. Rossin, F. Henneberger, and R. Zimmermann, Phys. Rev. B **54**, 4974 (1996).
[14] N. J. Traynor, R. T. Harley, and R. J. Warburton, Phys. Rev. B **51**, 7361 (1995).
[15] Y. Yamada, T. Sakashita, H. Wanabe, H. Kugimiya, S. Nakamura, and T. Taguchi, Phys. Rev. B **61**, 8363 (2000).
[16] J. M. Luttinger, Phys. Rev. **102**, 1030 (1956).
[17] R. Stepniewski, M. Potemski, A. Wysmolek, K. Pakula, J. M. Baranowski, Phys. Rev. B **60**, 4438 (1999).
[18] P. A. Shields, R. J. Nicholas, N. Grandjean, and J. Massies, Phys. Rev. B **63**, 245319 (2001).
[19] K. Müller and A. Schneider, Phys. Lett. **4**, 228 (1963).
[20] P. Lawaetz, Phys. Rev. B **4**, 3460 (1971).
[21] K. Oettinger, Al. L. Efros, B. K. Meyer, C. Woelk, and H. Brugger, Phys. Rev. B **52**, R5531 (1995).
[22] J. C. Miklosz and R. G. Wheeler, Phys. Rev. **153**, 913 (1967).